

P-V-T-X -fO₂ evolution from wolframite to sulphide depositional stages in intragranitic W-veins. An example from the Spanish Central System

ELENA VINDEL¹, JOSÉ ANGEL LOPEZ¹, MARIE-CHRISTINE BOIRON²,
MICHEL CATHELINÉAU² and ANGEL CARMELO PRIETO³

¹) Departamento de Cristalografía y Mineralología, Universidad Complutense,
28040 Madrid, Spain

²) CREGU, BP 23, and GS : CNRS-CREGU 077, 54501 Vandoeuvre lès Nancy, France

³) Departamento de Cristalografía y Mineralología, Universidad de Valladolid, Spain

Abstract: The relative P-T-X conditions of the deposition of wolframite and sulphides in quartz veins has been investigated using representative W-polymetallic sulphide veins hosted by peraluminous granites in the central domain of the Spanish Central System. Ore-bearing quartz veins fall into two groups : W-veins (wolframite-bearing quartz veins with minor amounts of sulphides) and sulphide (S) dominated veins (wolframite free). The two vein types (S and W) have similar orientation, silicate and sulphide mineralogy. A multidisciplinary approach based on a detailed fluid-inclusion analysis in relation with a paragenetic reconstruction of vein fillings suggests a similar genesis and fluid history, as follows :

(i) an early fluid stage, lacking in S-veins, characterized by CO₂-H₂O-NaCl rich vapours is at the origin of a strong K-mica alteration of the granite wall-rock, and of vein filling by milky quartz (QI) - phengite I - (wolframite), at around 130 ± 20 MPa and 525 ± 25°C ;

(ii) a second stage characterized by H₂O-CO₂-CH₄-NaCl fluids with a low volatile-phase density, at the origin of the deposition of : a) saccharoidal quartz (QII) (+ phengite II and minor amounts of scheelite in W-veins), and then, b) a chlorite-sulphide (pyrrhotite, sphalerite and galena) assemblage. A progressive decrease of the CO₂ content in fluids is recorded, CH₄ being the major volatile species in the latest inclusions spatially associated with sulphides. Pressure is around 130 ± 30 MPa, and temperature decreases from 380° to 330°C throughout the course of the fluid trapping.

iii) later fluid inputs in the veins are shown by two types of secondary aqueous fluid inclusions in healed micro-fissures, which display moderate Th (160°-220°C) and salinities.

The two main stages (wolframite, then sulphides) are characterized by a nearly isobaric cooling and dilution of volatile rich fluids. The X-fO₂ evolution indicates that fluid chemistry was probably controlled during the first stage by graphite-fluid equilibrium, implying a fluid source external to the granite (surrounding metamorphic series). The sulphide stage, which is ubiquitous in most W deposits, appears clearly in this example as the latest stage of a primary hydrothermal cycle involving volatile bearing fluids, and is not disconnected from the W stages.

Key-words : fluid inclusions, tungsten, sulphide, geothermobarometry, Spanish Central System.

Introduction

Wolframite is frequently associated with sulphides; although their genetic relationship is

often unclear, the latter is considered to be introduced during the late stages of ore deposition, as for instance in Panasqueira/Borralha, Portugal (Kelly & Rye, 1979; Noronha, 1984; Noronha *et*

al., 1992) or Grey River, Canada (Higgins, 1985). With the exception of Panasqueira, where fluids have been studied in the apatite coexisting with sulphides (Kelly & Rye, 1979) and some deposits from western Spain (Mangas & Arribas, 1987), very little is generally known of the fluid chemistry and of the conditions of sulphide deposition. The P-V-T-X conditions of wolframite and sulphide deposition have frequently been estimated using the fluids trapped as inclusions in quartz, although the relationships between different stages of fluid trapping and ore mineral deposition are frequently not fully established.

Typical sulphide quartz veins, with or without W minerals, from the same ore district have been studied with a special emphasis on the stages related to the late mineral assemblages, especially sulphides. They have been selected from the central sector of the Spanish Central System, the Cabeza Mediana-Collado zone, which hosts several W-polymetallic sulphide veins and provides a good opportunity to observe the relationships between these two kinds of mineralized quartz veins. Fluid inclusions have been studied as a function of the chronology of the vein infillings to decipher the P-T-X evolution of the different stages of W/S fluid migration.

Geology and mineralogy of the tungsten--sulphide veins

Geological setting of the studied area

The Spanish Central System is a northeast trending mountain chain located in the inner zone of the Hercynian Belt of Spain. The central part, called Sierra de Guadarrama, consists of granites and high-grade metamorphic rocks, mostly pre-Hercynian orthogneisses and some pre-Ordovician metasediments. The late Hercynian granites were emplaced from 345 to 275 Ma (Viallette *et al.*, 1981 ; Ibarrola *et al.*, 1988) after the main Hercynian orogenesis. They are mostly peraluminous monzogranites and leucogranites.

The granite batches intrude a complex metamorphic series characterized by a multistage Hercynian deformation and metamorphism. Most metamorphic rocks are metabasites and orthogneisses, but pre-Ordovician metapelitic intercalations are present. The actual thickness of the metasediments is not known, but it must be several kilometres thick. The most part of this series is formed by schists and paragneisses with

quartzites and discontinuous layers of marbles, amphibolites and calc-silicates rocks. Towards the top of the series some graphitic metapsammite bed outcrops are recognized (Bischoff *et al.*, 1973).

Vein-type W-sulphide mineralization accompanied by hydrothermal alteration is widespread in the central domain of the Spanish Central System. They have minor economic importance but were exploited during the second world war. The studied ore-bearing quartz veins can be divided into two groups : the W-S veins (wolframite-bearing quartz veins with minor amounts of sulphides) and the sulphide (noted S) dominated veins, which are wolframite free. Both are hosted by peraluminous granites and minor leucocratic granites. Sometimes, they cut across high-grade metamorphic rocks, usually orthogneisses or migmatites. In most cases, the veins are characterized by multistage ore deposition consisting of the successive crystallization of W (Sn-Mo) minerals and Cu-Zn-(Pb) sulphides (Vindel, 1980 ; Quilez *et al.*, 1990 ; Caballero *et al.*, 1992).

In the Cabeza Mediana area, the W/S quartz veins are hosted by a fine-grained cordierite-bearing peraluminous leucogranite. This granite belongs to an evolved late granite intrusion emplaced around 291 ± 6 Ma (Ibarrola *et al.*, 1988). It is a felsic PS-type granite with typical low Ba, Sr, Eu, Th, Y and REE and high W and U contents (Villaseca *et al.*, 1993). Frequently, the leucogranite is crosscut by porphyries dikes and aplites. The W/S quartz veins are irregular, relatively narrow (20-30 centimetres in width), strike N150°E to N-S, and are sub-vertical.

The sulphide quartz veins are similar in direction and width but have no observable wolframite, and an increased amount of sulphides. Both vein types occur either in the peraluminous granites or in the nearby Alpedrete monzogranite (Collado zone) which is a postkinematic calc-alkaline type intrusion surrounding the Cabeza Mediana granite.

Ore assemblages

The mineral assemblages of the two vein types were first described by Vindel (1980) and reveal a series of mineralizing stages separated in time by brecciation episodes. The dominant component of the veins is quartz, which can be separated on the basis of morphology and texture (in most of the veins) into : (1) a milky quartz (QI), and (2) a saccharoidal quartz (QII) with a mosaic-like texture.

	W-Sn Stage	Sulphide stage	Late stage
Phengite I, II	I	II	
Quartz I,II	I	II	
Chlorite			
Wolframite *			
Cassiterite *			
Fluorite *			
Scheelite *			
Pyrite			
Pyrrhotite			
Chalcopyrite			
Sphalerite			
Galena			
Melnikovite			
Covellite			
Cerussite			

Fig. 1. Paragenesis of W and S veins. Minerals specific to W veins are indicated by a star.

The textural and chronological relationships between ore, vein fillings and authigenic silicates have been established and are presented in Fig. 1. Three different depositional stages have been distinguished in all of the W-S veins.

(1) QI stage : the early quartz stage is responsible for strong K-mica (phengite I) alteration of the

granitic wall-rock. The alteration is restricted to a narrow zone adjacent to the veins (around a dm width). In W veins (Cabeza Mediana), wolframite is concentrated as irregular pods in QI together with minor amounts of cassiterite. Wolframite is not observed in S veins, although QI was present.

Table 1. Representative analytical data for the different groups of fluid inclusions

Type	Vc-w	Lw-c	Lw-m	Lw1	Lw2
Main components	H ₂ O-CO ₂ -(CH ₄)	H ₂ O-CO ₂ -CH ₄	H ₂ O-CH ₄	H ₂ O-NaCl	H ₂ O-NaCl
Occurrence	Isolated in QI	Isolated in QII Secondary in QI	Isolated in QII Secondary in QI	Secondary in QI-QII	Secondary in QI-QII
Habitus at room T °C	Three phases	Two phases	Two phases	Two phases	Two phases
Gas infilling	0.5 - 0.9	0.4 - 0.5	0.3 - 0.5	0.1 - 0.3	0.1 - 0.25
Tm CO ₂ (°C)	-58 / -60 mode : -58.6				
Tm ice (°C)	-1.2 / -3.8 mode : -1.5	-2 / -7 mode : -3.3	-0.9 / -6 mode : -2.9	-1.5 / -5.7 mode : -3.1	-0.2 / -1.5 mode : -0.6
Tm cl (°C)	7.6 / 11.5 mode : 9.3	7.6 / 9 mode : 8.5	7 / 16 mode : 8.6		
Th CO ₂ (°C)	7.8 / 17.3 mode : 17 (V)				
TH (°C)	310 / 340 mode : 330 (V)	290 / 380 mode : 300 (L(V))	210 / 370 mode : 290 (L)	155 / 230 mode : 200 (L)	135 - 210 mode : 190 (L)
Salinity (wt % eq. NaCl)	0.2 - 1.8	0.2 - 2.2	0.1 - 2.0	2.6 - 8.8	0.3 - 2.6
H ₂ O mole %	75 - 90	93 - 95.5	87 - 94	91.2 - 97.4	97.4 - 99.7
CO ₂ mole %	9 - 20	1.3 - 4.3	nd		
CH ₄ mole %	0.2 - 3	0.3 - 4.1	4.9 - 12.6		
N ₂ mole %	nd	nd - 1.1	nd		

Tm CO₂ : melting temperature of CO₂ ; Tm ice : melting temperature of ice ; Tm cl : melting temperature of clathrate ; Th CO₂ : homogenization temperature of CO₂ ; Th : global homogenization temperature. L : Liquid, V : Vapor ; nd : not detected. All temperatures are given in °C.

Table 2. Raman data and interpreted bulk composition of selected fluid inclusions. Vein type : W or S refer to wolframite or sulphide veins respectively.

			Microthermometry						Raman data			Bulk composition					
Inclusion types	Vein type	Flw	Flc	TmCO ₂	Th CO ₂ (V)	Tmcl	TmH ₂ O	Th	ZCO ₂	ZCH ₄	ZN ₂	XH ₂ O	XCO ₂	XCH ₄	XN ₂	XNaCl	Density
	Inclusion n°																
Vc-w	W-3	0.40	0.15	-58.1	16.1	7.6	nv	310 (d)	94.1	5.9	nd	84.8	13.5	0.7	0	1	0.54
Lw-c	W-4	0.50	0.50	nv	nv	8.6	nv	294 (d)	66.8	33.2	nd	95.1	2.9	1.4	0	0.6	0.56
Lw-c	W-6	0.60	0.40	nv	nv	8.8	nv	327	18.3	64.3	17.4	92.3	1.3	4.1	1.1	1.2	0.63
Lw-c	W-7	0.50	0.50	nv	nv	7.6	nv	381	56.2	43.8	nd	92.5	3.0	2.4	0	2.5	0.55
Lw-c	S-9	0.50	0.50	nv	nv	7.7	-3.1	397	64.9	35.1	nd	95.8	2.5	1.4	0	0.3	0.55
Lw-c	S-10	0.50	0.50	nv	nv	8.5	-3.5	290(d)	57.5	33.3	7	94.3	2.9	1.7	0.3	0.8	0.55
Lw-c	S-17	0.60	0.40	nv	nv	8.3	nv	nv	76.0	5.3	18.5	93.5	4.3	0.3	1	0.9	0.65
Lw-m	W-8	0.60	0.40	nv	nv	12.1	nv	287	nd	100	nd	89.7	0	9.2	0	1.1	0.64
Lw-m	S-11	0.60	0.40	nv	nv	15.9	-2.7	288	nd	100	nd	86.8	0	12.6	0	0.6	0.65
Lw-m	S-12	0.60	0.40	nv	nv	10.3	-3.9	308	nd	100	nd	90.6	0	8.1	0	1.3	0.63
Lw-m	S-13	0.70	0.30	nv	nv	8.3	-1.5	246	nd	100	nd	93.9	0	5.5	0	0.6	0.71
Lw-m	S-14	0.70	0.30	nv	nv	8.8	-0.8	215	nd	100	nd	94.1	0	5.6	0	0.3	0.71
Lw-m	S-16	0.70	0.30	nv	nv	8.6	nv	371	nd	100	nd	94.3	0	5.4	0	0.3	0.71

Tm CO₂ : melting temperature of CO₂ ; Tm ice : melting temperature of ice ; Tm cl : melting temperature of clathrate ; Th CO₂ : homogenization temperature of CO₂ ; Th : global homogenization temperature. V : Vapor ; nd : not detected, nv : not visible, d : decrepitated inclusion. All temperatures are given in °C.

(2) QII stage : saccharoidal quartz (QII) is associated with a late crystallization of phengite (phII). This quartz bears minor amounts of scheelite (\pm fluorite), which is an *in-situ* replacement of wolframite.

Pyrite, chalcopyrite and sphalerite, chlorite (\pm pyrrhotite) are typically late and fill cavities and fractures in the wolframite. Sulphides also occur as disseminated inclusions trapped within the quartz II during its crystallization, especially in S-veins. Chalcopyrite and sphalerite are usually intimately associated, the chalcopyrite containing "star-like" sphalerite inclusions. Galena was only observed in S-veins from Collado.

(3) Late, low-temperature assemblages (melnikovite/covellite; cerussite/covellite) replace locally the previous sulphide assemblages.

Analytical methods

Primary or secondary fluid inclusions were found within the two main types of quartz. No suitable inclusions were found in scheelite, fluorite, or sphalerite. The succession of fluid trapping has been studied by looking at the textural relationships between fluid inclusions, their host mineral, microstructures, and the ore minerals.

Microthermometric characterization of the fluids was undertaken using a heating-freezing Chaixmeca stage (Poty *et al.*, 1976). The stage was calibrated at high temperature with melting

point standards and at low temperature with a pure natural CO₂ fluid inclusion at the triple point (-56.6°C) and the melting point of toluene (-95°C). The accuracy of measurements is considered to be $\pm 0.1^\circ\text{C}$ at low temperature and about $\pm 0.5^\circ\text{C}$ at the maximum temperatures reached in this study (400°C). Salinity is expressed in equivalent wt% NaCl (Bodnar, 1993) and fluid density (Potter, 1977) of volatile-free inclusions in quartz were determined by microthermometry. In high dense volatile fluid inclusions, CO₂ was identified by the melting of a solid below -56.6°C. In inclusions with low density volatile phase, the presence of a volatile phase (CO₂ or CH₄) was identified by the melting of hydrates in favourable cases, or by Raman microprobe. The salinity of the CO₂/CH₄ rich inclusions was calculated from the temperature of clathrate dissociation, the melting temperature of ice and the Raman gas analyses, using the computer code of Dubessy *et al.* (1992). The volumetric fraction of the aqueous liquid (Flw) and the volatile-rich phase (Flc) were estimated by reference to the volumetric chart of Roedder (1972).

The composition of the non-aqueous portion of individual inclusions was measured using a Dilor X-Y multichannel modular Raman spectrometer (at CREGU). Bulk composition and molar volume were computed from the P-V-T-X properties of individual inclusions in the C-O-H-(N-S) system (Dubessy, 1984 ; Dubessy *et al.*, 1989, 1992 ; Thiery *et al.*, 1994).

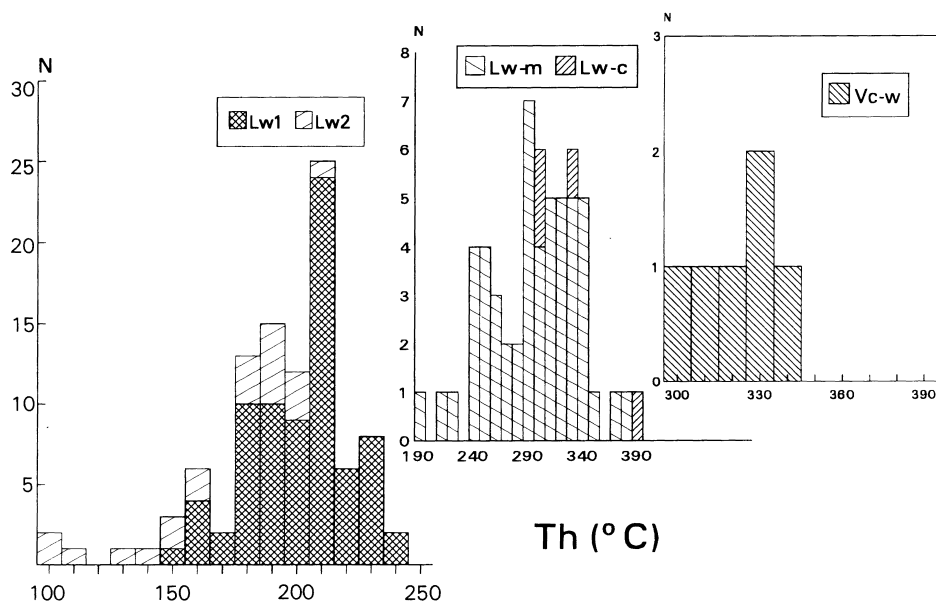


Fig. 2. Histograms of global homogenization temperatures for Lw1, Lw2, Lw-m, Lw-c and Vc-m fluid-inclusion types.

Mineral geothermobarometry was carried out on phengite (phI and phII) and chlorite samples from W and S-veins using crystal chemical data. Systematic analysis of chlorites and phengites was carried out using a Camebax electron microprobe (Nancy I University) with the following analytical conditions: 15 kV acceleration voltage, 10 s counting time, 10 nA excitation current, correction programme PAP. The following minerals were used as standards: corundum (Al), albite (Na), orthoclase (Si), hematite (Fe), apatite (Ca), KTiPO_5 (K), forsterite (Mg), rutile (Ti), rhodonite (Mn) and chromite (Cr). The maximum analytical error was 3 % of the total. Crystallization temperatures have been estimated using the geothermometers of Velde (1965) and Cathelineau (1988) for K-micas and chlorite, respectively.

Fluid-inclusion data

Fluid inclusions were systematically studied in wafers from quartz QI and QII sampled in the W-S and S-veins. About 250 microthermometric results are summarized in Table 1 and Raman microprobe analyses carried out on selected fluid inclusions are given in Table 2.

In the discussion of fluid-inclusion data, the

following nomenclature has been adopted. Where homogenization is to the liquid (L) or vapour (V) phase, L or V is used to signify the mode of homogenization. The presence of H_2O is signified by subscript (w), C-H-O-(N-S) species by (c), and CH_4 by (m). The order of the various subscripts takes into account the relative abundance of volatile species. The L (or V) c-w inclusions correspond to the H_2 type in the Van den Kerkhof (1988) classification.

Volatile-rich inclusions

Three types, Vc-w, Lw-c and Lw-m have been distinguished on the basis of the microthermometric and Raman data. The Vc-w inclusions are exclusively observed in W-veins. The Lw-c and Lw-m inclusions display similar succession and relationships with the host quartz types in the two vein types. As the general microthermometric features of Lw-c and Lw-m inclusions found in W-S and S types are the same, they have not been distinguished in the presentation. Only the selected representative inclusions studied both by microthermometry and Raman have been discriminated according to the vein type.

Vc-w inclusions are extremely scarce and found exclusively as isolated inclusions in QI

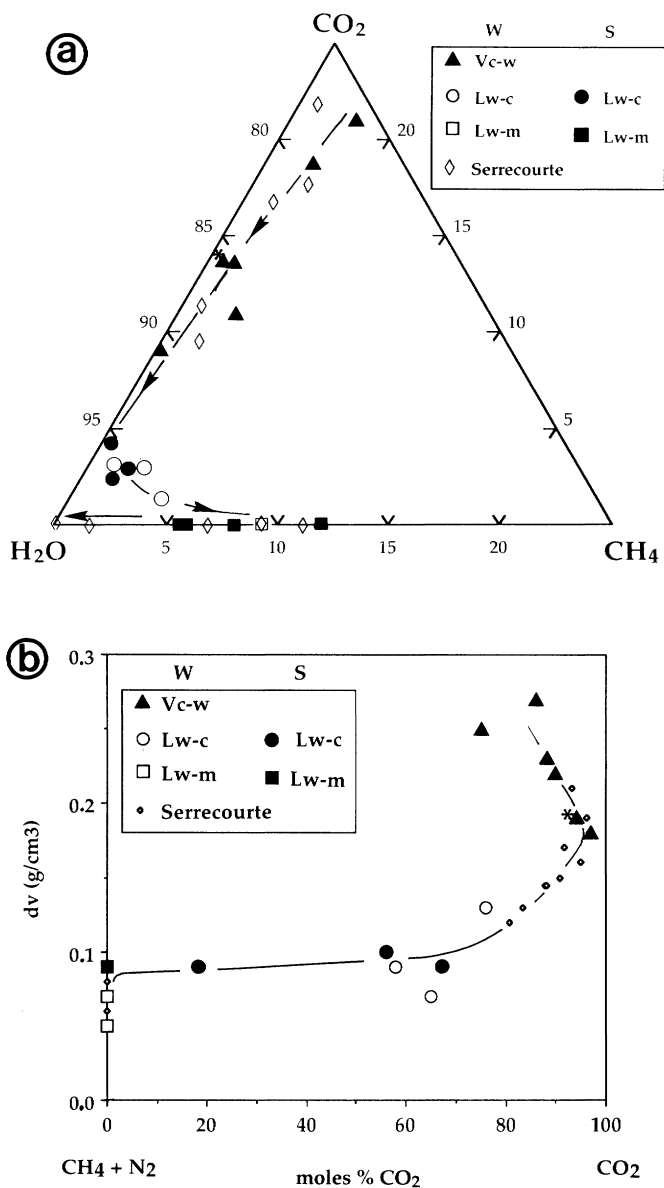


Fig. 3. Summary of the evolution of the bulk composition (a : CO_2 - CH_4 - H_2O ternary plot), and of the volatile density (d_v vs. ZCO_2 :b) of type Vc-w, Lw-c and Lw-m fluid inclusions. W = W-veins ; S = Sulphide veins. The data from Serrecourte W quartz veins (Ramboz *et al.*, 1985) have been plotted for comparison. Among the analytical points for the Vc-w type, the star (*) pinpoints the data corresponding to the inclusion W-3 from Table 2.

from the W-veins. They exhibit three phases at room temperature, H_2O (L), CO_2 (L) and CO_2 (V). CO_2 homogenizes to the vapour phase in the range 7.8/17.3°C. Melting temperature of CO_2

(TmCO_2) is significantly lower than the Tm of pure CO_2 , in the range -58/-60°C , with a mode around -59°C, due essentially to the presence of CH_4 as confirmed by Raman analysis (no N_2

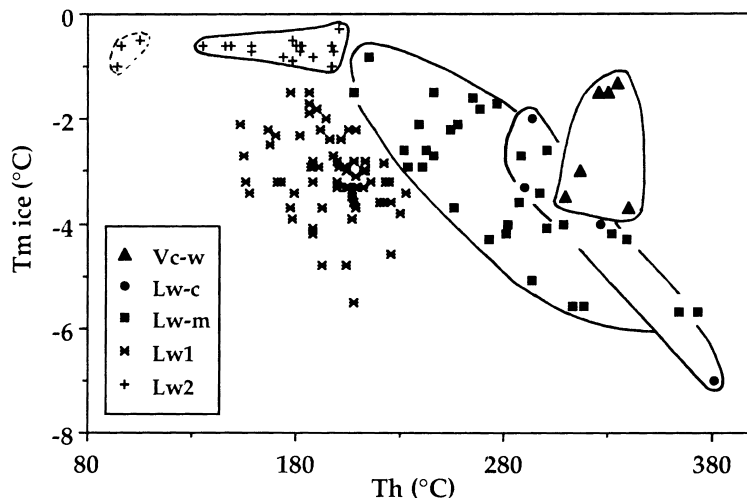


Fig. 4. Homogenization temperature (Th) vs. ice melting temperature (Tm ice) plot for all studied fluid-inclusion types.

detected). Unfortunately, only one representative inclusion of sufficient size could be studied by Raman (Table 2). Thus, compositions have been estimated on the basis of the microthermometric data (Tm CO₂, Th CO₂, Tm ice and Tm cl) in the CO₂-CH₄-H₂O (NaCl) system. The melting temperature of clathrate (Tm cl) is in the range 8.3/12°C and the melting temperature of ice (Tm ice) is in the range -1/-4°C with a mode around -3°C. Vc-w inclusions homogenize between 290 and 330°C.

Lw-c inclusions are two-phase at room temperature, randomly distributed, and considered as primary in QII. In QI W-veins, they occur along healed fractures and are considered to be secondary. Lw-m inclusions are two-phase at room temperature, and mostly spatially associated with sulphides but are also found in fluid-inclusion planes (FIP) in earlier quartz. Both types are ubiquitous in all samples and vein types, but Lw-m are dominant in S-veins. Raman microprobe analysis shows that Lw-c inclusions have a large variation in the CH₄/CO₂ ratio. In Lw-m inclusions, the volatile phase is entirely dominated by CH₄. The Tm cl range is larger for Lw-m inclusions (7/16°C) than for Lw-c inclusions (7/9°C) due to the increase of the CH₄ content. The global homogenization is to the liquid phase and is significantly higher for Lw-c inclusions (290-380°C) than in Lw-m inclusions (210-370°C) (Fig. 2), although decrepitation sometimes occurs before homogenization.

Aqueous fluids

Lw1 and Lw2 inclusions contain two fluid phases, are irregularly shaped, occur along secondary healed fracture planes in QI and QII and postdate the other inclusion types. They are not abundant. The typology of aqueous fluid inclusions was based on Tm ice-Th pairs, and textural relationships.

Lw1 fluid inclusions are characterized by moderate salinities, with Tm ice between -1.5 and -5.7°C (mode around -3°C) corresponding to a salinity of 2.6 to 8.8 wt. % eq. NaCl, and moderate Th(L), ranging from 130 to 290°C (mode around 210°C).

Lw2 fluid inclusions are clearly later than Lw1 and have higher Tm ice in the range -0.2 to -1.5°C (mode around -0.6°C) corresponding to a low salinity of 0.3 to 2.6 wt.% eq. NaCl. Th(L) is in the range 90- 210°C (mode around 190°C). No C-H-O-(N-S) species were detected by Raman microprobe in the non-aqueous portion of the Lw1 and Lw2 inclusions.

Although the careful examination of the fluid-inclusion shapes does not give argument for clear post-trapping changes affecting the inclusions, the necking down process cannot be precluded to explain the rather wide scattering of Th for a given range of Tm ice.

Bulk chemical evolution

The bulk composition of the selected fluid

inclusions Vc-w, Lw-c and Lw-m are given in Table 2. The evolution of the fluid composition during these volatile bearing fluid stages is illustrated by a $\text{CO}_2\text{-CH}_4\text{-H}_2\text{O}$ ternary plot (Fig. 3a), and by Fig. 3b which shows the density evolution as a function of XCO_2 . Some literature data have been considered for comparison, especially from a Hercynian quartz-wolframite vein from the French Massif Central (Serrecourte vein), for which a detailed Raman and microthermometric study is available (Ramboz *et al.*, 1985).

The three volatile-bearing fluid inclusion types exhibit a compositional trend from Vc-w, Lw-c, to Lw-m inclusions characterized by : i) a decrease of the density, and volume fraction of the volatile phase, ii) first a slight increase, followed by a rather strong decrease of XCO_2 in favour of XCH_4 which is the only species detected in the volatile phase of Lw-m inclusions.

No significant difference characterizes the fluids found in W or S veins. The similarity with the trend depicted at Serrecourte by Ramboz *et al.* (1985) is noteworthy, especially the density ranges for the transition stages from Lw-c to Lw-m fluids. However, the dominant fluid inclusions found at Cabeza Mediana-Collado show compositions dominated by the intermediate volatile phase compositions (20 to 80 % $\text{Z CH}_4 + \text{N}_2$), the early stages being represented by scarce inclusions.

The Th-Tm ice (Fig. 4) plot shows a progressive decrease of Th and salinity in the volatile-rich fluids. The evolution of volatile rich (Vc-w, Lw-c, Lw-m) and volatile free (Lw1-Lw2) fluid types is peculiar. Considering the Lw-m trend, the Th decrease at decreasing Tm ice indicates a probable mixing of the aqueous part of the early fluid by a more dilute and cooler end-member. The lack of clear decrease in XCH_4 in the dilution process may result either from analytical difficulties (water content estimate), or from a lack of contrasted XCH_4 in the two end-members.

Lw-m and Lw1 inclusions display two distinct evolutions at decreasing Th and salinities without any clear evidence of mixing between the two types. The Lw2 type could be eventually considered as a possible end-member of the dilution trend that characterizes the Lw1 type. However, the general features of the fluids suggest several independent fluid inputs in the veins.

Observed trends reflect that dilution and cooling characterize the whole evolution of the sys-

tem, during a succession of distinct fluid events. These processes are similar to those already documented by Mangas & Arribas (1987, 1988) on other W-Sn deposits from western Spain.

P-T reconstruction

Mineral geothermometry

Electron microprobe analyses have been carried out on K-micas (PhI and PhII) and on

Table 3. Statistic treatment of structural formulae (half formulae) of phengite I (W-veins), phengite II (W-S and S-veins) and chlorite, with indication of the mean, standard deviation (in parenthesis), minimum and maximum.

	Chlorite	Phengite I	Phengite II
Si	2.77 (0.03) 2.73 - 2.83	3.10 (0.03) 3.01 - 3.15	3.16 (0.04) 3.09 - 3.23
Al ^{IV}	1.22 (0.03) 1.17 - 1.27	0.90 (0.03) 0.85 - 0.99	0.83 (0.04) 0.77 - 0.91
Al ^{VI}	1.47 (0.04) 1.40 - 1.52	1.85 (0.03) 1.76 - 1.91	1.81 (0.03) 1.78 - 1.87
Fe	2.76 (0.12) 2.44 - 2.93	0.10 (0.02) 0.07 - 0.16	0.12 (0.02) 0.08 - 0.14
Mg	1.53 (0.13) 1.36 - 1.85	0.09 (0.02) 0.05 - 0.17	0.11 (0.02) 0.08 - 0.14
Mn	0.06 (0.02) 0.03 - 0.10	0 (0) 0 - 0.02	nd
R ²⁺	4.38 (0.60) 4.30 - 4.52	0.19 (0.04) 0.11 - 0.36	0.24 (0.04) 0.16 - 0.30
Fe/(Fe + Mg)	0.62 (0.2) 0.56 - 0.67	0.55 (0.08) 0.33 - 0.66	0.53 (0.05) 0.45 - 0.62
Vacancy	0.14 (0.03) 0.08 - 0.19		
Ca		nd	nd
Na		0.05 (0.01) 0.03 - 0.07	0.04 (0.02) 0.02 - 0.09
K		0.89 (0.03) 0.80 - 0.93	0.82 (0.03) 0.78 - 0.87
I C		0.89 (0.04) 0.84 - 1.00	0.86 (0.05) 0.80 - 0.96

nd : not detected, IC : Interlayer charge.

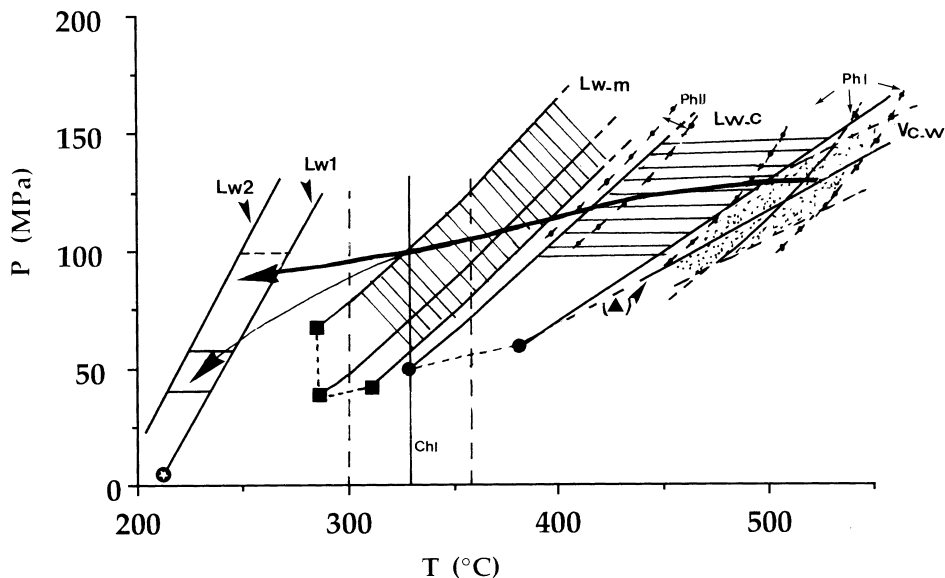


Fig. 5. P-T reconstruction of conditions prevailing for the W-polymetallic sulphide with indication of representative isochores and data from mineral geothermometers. For a given volatile-rich fluid type, only extreme isochores and their related Ph-Th pair (symbols) have been drawn, as well as the most probable trapping P-T domain which is identified by a specific pattern (dots for Vc-w, horizontal hachures for Lw-c, and slanting hachures for Lw-m). For Lw1 and Lw2 inclusions, only mean isochores have been drawn. The P-T curves for phengites I and II (noted PhI and PhII) are reported from Velde data (1965), as well as the mean value and the range of the temperature estimate for chlorite (ChI). Symbols are the same as in Fig. 3.

chlorites (ChI) in samples where they have not been affected by supergene alteration. Table 3 shows the results of selected microprobe analyses.

Phengites

The structural formulae of K-micas have been calculated on the basis of 11 oxygens (half formula). They are considered to be phengites according to Velde (1965). The crystal-chemistry of the K-micas is characterized by : i) a Si content around 3.10 ± 0.03 for phengite I and 3.16 ± 0.04 for phengite II ; ii) a rather constant octahedral substitution of Al by divalent cations (Mg^{2+} and Fe^{2+}) for phI and phII (0.07 - 0.15), and iii) an interlayer charge ranging between 0.80 to 1.0, with minor amounts of Na reaching 0.01 to 0.09 per half formula.

P-T reconstruction of conditions prevailing for phengite I and II (Fig. 5) have been established according to Velde (1965), as no further indications could be obtained for the low pressure

range (< 1.5 kbar) from the data of Massonne & Schreyer (1987). The estimates obtained have to be used with caution since the geothermometer is based on few experimental data in the low-P low-T range, and for Mg-phengites. However, the results seem to be compatible with a reasonable estimate of the general P-T evolution that can be inferred for such a geological context.

Chlorites

The structural formulae of chlorites have been calculated on the basis of 14 oxygens (half formula). They show a $Fe/(Fe + Mg)$ ratio of 0.62 ± 0.02 . Using the revised Cathelineau's chlorite geothermometer (1988), a temperature of $330 \pm 15^\circ C$ is estimated for the chlorite-sulphide depositional stage. The consideration of the different chemical variables and other geothermometric tools (De Caritat *et al.*, 1993) does not provide any additional constraints and confirms that chlorite display features typical of relatively high temperature conditions ($> 250-300^\circ C$).

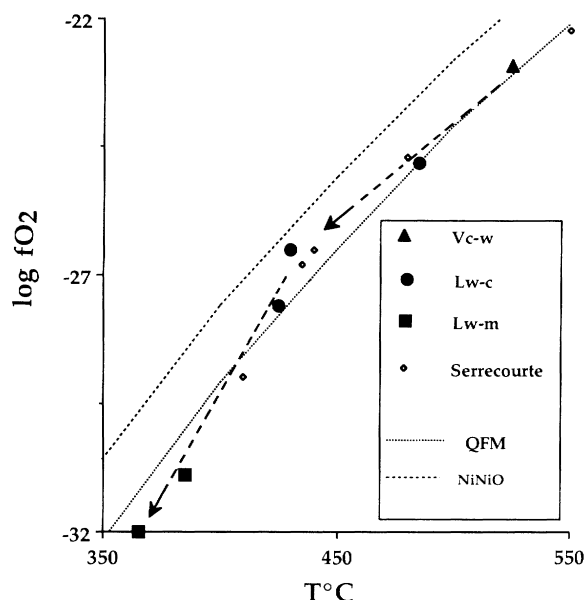


Fig. 6. Log f_{O_2} -T evolution along the P-T path determined in Fig. 5. The data from Serrecourte W quartz veins (Ramboz *et al.*, 1985) have been plotted for comparison.

P-T estimation

The P-V-T-X properties of aqueous carbonic inclusions were modelled for the system H_2O - CO_2 - CH_4 using the state equations of Kerrick & Jacobs (1981) and Jacobs & Kerrick (1981). The data are given in Table 2. For aqueous inclusions, the isochores have been drawn in the H_2O -NaCl system using the data from Zhang & Frantz (1987). Representative isochores are given in Fig. 5 together with the temperature estimates from the mineral geothermometers. For an error of 10 % on the estimation of the water content of volatile rich inclusions, the uncertainty in the P estimate from an isochore (at a given temperature) is considered to be around ± 20 MPa (Cathelineau *et al.*, 1993).

QI-W-stage

Minimal P-T conditions of trapping are constrained by the homogenization P-T pair (Ph-Th) which is $325 \pm 15^\circ C$, 80 ± 10 MPa. Considering that K-micas are synchronous of Vc-w fluids, the intersection of isochores with the P-T curve for the $Si_{3.10}$ phengite (PhI) gives a rough estimate of the P-T conditions for the deposition of wolframite, *e.g.* $525 \pm 25^\circ C$, 130 ± 20 MPa. This pressure is probably higher than the hydrostatic

pressure, and close to the lithostatic pressure. If lithostatic, such a pressure may indicate a relatively deep structural level (4-6 km depth assuming an average density of 2.6 for the rock column).

QII-stage

Minimal trapping conditions (Ph-Th) for Lw-c fluids are : $350 \pm 20^\circ C$; 50 ± 5 MPa. Considering the data for phII, which are synchronous with QII, and assuming that the pressure probably did not exceed the pressure of the preceding stage, the trapping P-T pair is estimated to be around : $380 \pm 40^\circ C$; 130 ± 30 MPa.

Sulphide stage

Minimal trapping conditions (Ph-Th) for Lw-m fluids are : $260 \pm 20^\circ C$; 50 ± 20 MPa. Considering the estimated crystallization temperature of chlorite ($330 \pm 15^\circ C$), which probably crystallized in association with the sulphides, the probable trapping conditions were around $330 \pm 30^\circ C$ and 100 ± 20 MPa. Pressure conditions are therefore similar to the preceding stage.

Late stages

Finally, high-density aqueous fluids related to

the latest stages have probably been trapped at a pressure which could be bracketed between the sublithostatic pressures of the preceding stage (100 ± 20 MPa) and the corresponding hydrostatic pressure (40 ± 10 MPa, taking by simplification a water column with a density of 1) at the same structural level (around 4 ± 1 km depth), if no uplift had occurred (arrows for both cases in Fig. 5). Temperatures in both cases (lithostatic or hydrostatic pressures) are within the range of $240 \pm 30^\circ\text{C}$.

The general fluid evolution implies first a dilution of a volatile-rich fluid by cooler fluids of aqueous composition. Slight changes in the fluid-pressure regime around the lithostatic pressure (fluid pressure fluctuation, or slight change in the structural level) could be inferred for the three first fluid types.

Redox conditions

The P-T-fO₂ relationships calculated for the different types of fluids indicate that the fO₂ was around (or slightly above for some Lw-c type inclusions) the fO₂ fixed by the Q-F-M oxygen buffer, for the two first fluid types, Vc-w and Lw-c (Fig. 6). Considering the lack of magnetite (and fayalite) in the nearby environment of the veins, the above mentioned values suggest that fO₂ was buffered by equilibrium with graphite, as confirmed by the calculation of the P-T-fO₂ values computed from the graphite-fluid equilibrium using the equation of state from Kerrick & Jacobs (1981). Fluid-graphite equilibrium was probably reached in the surrounding metamorphic formation, suggesting the lack of equilibration between the fluid and the granite assemblages, and that the source for volatile components was external to the granite.

For the intermediate compositions showing increasing CH₄ content up to the disappearance of detectable CO₂ in Lw-m fluids, the fO₂ is much lower. That means that the fluid chemistry has not longer been controlled by graphite at the late stages of fluid migration. The observed drop in fO₂ may indicate that the temperature of the fluid system was too low to maintain equilibrium with graphite. The minimum blocking temperature of 370°C deduced from other natural examples (Serrecourte, Ramboz *et al.*, 1985) is remarkably similar to the temperature drop inferred for the Lw-c to Lw-m transition (around 100 MPa) in the studied veins.

Metallogenic implications

The deposition of wolframite is probably related to Vc-w fluids and QI crystallization. Similar relationships between CO₂-CH₄ rich fluids and W mineralization is frequently encountered in Hercynian quartz veins from western Europe (Noronha, 1974; Kelly & Rye, 1979; Ramboz, 1980; Ramboz *et al.*, 1985; Durisova *et al.*, 1979; Aissa *et al.*, 1987; Mangas & Arribas Jr., 1987) and Morocco (Cheilletz, 1984; Giuliani, 1984). Crushing of wolframite within glycerine under a microscope clearly indicates the presence of volatile compounds in inclusions in this mineral. It is difficult to relate precisely the deposition of wolframite at Cabeza Mediana to changes in P-T-X conditions, due to the scarcity of available fluid inclusions. However, it is likely to consider that dilution and temperature decrease, which cause an increase of the dielectric constant of the fluid and correlatively the destabilization of neutral species, may cause the wolframite precipitation, as already inferred by Ramboz *et al.* (1985) and Dubessy *et al.* (1987).

The replacement of wolframite by scheelite can be related to the first stage of QII crystallization. During this period, the fluid was a low-density, CO₂-CH₄ rich volatile phase at a temperature of $340\text{--}420^\circ\text{C}$. Other studies have documented similar fluids such as at the Felbertal deposit (Schenk *et al.*, 1990), or the Orlik deposit (Durisova *et al.*, 1992). In the Cabeza Mediana vein, the drop in temperature seems to be the most likely factor to account for the change in the CH₄/CO₂ ratio, departing from graphite-fluid equilibrium below 400°C . The increase in the water content indicates the influx of a distinct fluid component which may have been sufficiently enriched in Ca to stabilize scheelite at the expense of wolframite.

The close relationship between CH₄-bearing inclusions and sulphides, especially their abundance in the sulphide-bearing quartz veins, as opposed to the W veins, indicates a relatively early crystallization of sulphides from the CH₄-bearing fluids. The lack of detectable CO₂ in this fluid, and the presence of a stable pyrite/pyrrhotite assemblage indicates that the sulphides crystallized under low fO₂-fS₂ (fO₂ < 10^{-34} ; fS₂ $\approx 10^{-12}$ at 330°C). The main precipitation mechanism could be a dilution process as shown by the decreasing salinity with decreasing Th shown by the Lw-m inclusions. In this case, sulphide deposition is not related to volatile-free fluids, such as those de-

scribed at Panasqueira (Kelly & Rye, 1979), where, however, the aqueous liquids are related to the crystallization of apatite which is later than the sulphide stage of mineralization.

The late fluids (aqueous liquids Lw1 and Lw2) document further relatively limited fluid migration along the fault zones, which could be related to slight tectonic reactivation (microfissure opening) and produced the latest sulphide crystallization or replacement.

Conclusions

The Cabeza Mediana-Collado W/S quartz veins record a rather detailed evolution of the fluid migration stages at the origin of W/S mineral assemblage deposition. The detailed study of fluid inclusions in relation to the sequence of mineral deposition yields significant constraints on the P-T-X conditions of ore deposition :

- the P-T path is characterized by a nearly isobaric evolution during the early stages dominated by the volatile-rich inclusions.

- the X-fO₂ evolution indicates that fluid chemistry was controlled by graphite-fluid equilibrium, implying a source for fluids external to the granite (surrounding metamorphic series) and possibly also for W. The temperature changes and the dilution of the volatile-bearing fluids by cooler aqueous fluids is responsible for fluid disequilibrium with graphite and the subsequent CH₄-dominated low-density volatile component in the fluids. Rather similar features characterize the Au-As bearing veins from western Europe (Boiron *et al.*, 1990, 1993) where fluids equilibrated at relatively high temperature with metamorphic rocks are progressively diluted by low-temperature aqueous fluids. There is no evidence of magmatic contribution, contrary to that shown in other zone of the Central System by the presence of high-temperature brines (Quilez *et al.*, 1991, Quilez, 1994) associated with the earliest alteration mineral assemblage (muscovite-K feldspar-garnet zone).

- the sulphide stage, which is ubiquitous in most W deposits but not systematically described in detail, is exemplified by the W/S veins from the Cabeza Mediana-Collado area. It appears during the latest stage of hydrothermal circulation involving volatile-bearing fluids, and is related to the W mineralization. Both two vein types (S and W) display similar orientation, sil-

icate and sulphide mineralogy, and P-T-X conditions, indicating a similar genesis and fluid history. The main difference lies in the better expression of one of the stage over the others (Vc-w fluid stage with W deposition in W veins; Lw-m fluid stage with sulphides in S veins), this being probably the result of local differences in the vein opening history.

- dilution and cooling characterize the whole evolution of the volatile-rich fluid stages (main depositional stage). However, evidence for later fluid input is given by aqueous fluids (Lw1, Lw2) trapped in healed cracks which are not related to the main depositional stage.

Acknowledgements : This work has been supported by the "Accion Integrada Francia-España PICASSO " and by the CEC programme "Human Capital and Mobility" (network HCM, CEE-XII G - Contract CT 930198 - PL 922279): "Hydrothermal /metamorphic water rock interactions in crystalline rocks : a multidisciplinary approach based on paleofluid analysis". J. Dubessy, D. Banks and J. Mangas are warmly thanked for the review of the manuscript, and their suggestions.

References

- Aissa, M., Weisbrod, A., Marignac, C. (1987) : Caractéristiques chimiques et thermodynamiques des circulations hydrothermales du site d'Echassières. *Mém. GPF 1, Géol. de la France*, **2-3**, 335-350.
- Bischoff, L., Schaffer, G., Schmidt, K., Walter, R. (1973) : Zur Geologie der mittleren Sierra del Guadarrama (Zentral Spanien). *Münster Forsch. Geol. Paläontol.*, **28**, 1-27.
- Bodnar, R.J. (1993) : Revised equation and table for determining the freezing point depression of H₂O-NaCl solutions. *Geochim. Cosmochim. Acta*, **57**, 683-684.
- Boiron, M.C., Cathelineau, M., Dubessy, J., Bastoul, A. (1990) : Fluids in hercynian Au-veins from the variscan belt. *Mineral. Mag.*, **54**, 231-243.
- Boiron, M.C., Essarraj, S., Barakat, A., Castroviejo, R., Cathelineau, M., Noronha, F., Nogueira, P., Yardley, B., Banks, D., Marignac, C., Pereira, E., Urbano, R., Florido, P., Garcia Palomero, F. (1993) : P-V-T-X changes throughout the formation of intragranitic Au concentration in the northwestern iberian massif (Spain- Portugal): an integrated fluid inclusion study. *Proc. of the second biennial SGA meeting*, Fenoll Hach-Ali, Torres Ruiz and Gervilla ed., 605-608.

- Caballero, J.M., Casquet, C., Galindo, C., Gonzalez Casado, J.M., Lopez Garcia, J.A., Quilez, E., Sierra, J., Vindel, E. (1992) : La Sierra de Guadarrama : un ejemplo de actividad hidrothermal recurrente en el tiempo y en el espacio. *Actas III, Congreso Geológico de España*, **T3**, 42-45.
- Caritat, de P., Hutcheon, I., Walshe, J.L. (1993) : Chlorite geothermometry : a review. *Clays & Clay Minerals*, **41**, 219-239.
- Cathelineau, M. (1988) : Cations site occupancy in chlorites and illites as a function of temperature. *Clay Minerals*, **23**, 471-485.
- Cathelineau, M., Boiron, M.C., Essarraj, S., Dubessy, J., Lespinasse, M., Poty, B. (1993) : Fluid pressure variations in relation to multistage deformation and uplift : a fluid inclusion study of Au quartz veins. *Eur. J. Mineral.*, **5**, 107-121.
- Cheilletz, A. (1984) : Caractéristiques géochimiques et thermobarométriques des fluides associés à la scheelite et au quartz des minéralisations de tungstène du Jbel Aouam (Maroc Central). *Bull. Minéral.*, **107**, 255-272.
- Dubessy, J. (1984) : Simulation des équilibres chimiques dans le système C-O-H. Conséquences méthodologiques pour les inclusions fluides. *Bull. Minéral.*, **107**, 155-168.
- Dubessy, J., Ramboz, C., Nguyen Trung, C., Cathelineau, M., Charoy, B., Cuney, M., Leroy, J., Poty, B., Weisbrod, A. (1987) : Physical and chemical controls (fO₂, T, pH) of the opposite behaviour of U and Sn-W as exemplified by hydrothermal deposits in France and Great Britain, and solubility data. *Bull. Minéral.*, **110**, 261-281.
- Dubessy, J., Poty, B., Ramboz, C. (1989) : Advances in the C-O-H-N-S fluid geochemistry based on micro-Raman spectroscopic analysis of fluid inclusions. *Eur. J. Mineral.*, **1**, 517-534.
- Dubessy, J., Thiery, R., Canals, M. (1992) : Modelling of phase equilibria involving mixed gas clathrates : Application to the determination of molar volume of the vapour phase and salinity of the aqueous solution in fluid inclusions. *Eur. J. Mineral.*, **4**, 873-884.
- Durisova, J., Charoy, B., Weisbrod, A. (1979) : Fluid inclusion studies in minerals from tin and tungsten deposits in the Krusne Hory Mountains (Czechoslovakia). *Bull. Minéral.*, **102**, 665-675.
- Durisova, J., Sztacho, P., Dubessy, J. (1992) : A fluid inclusion study of Au-W stratiform mineralization at Orlik near Humpolec, Czechoslovakia. *Eur. J. Mineral.*, **4**, 965-976.
- Giuliani, G. (1984) : Les concentrations filoniennes à tungstène-étain du massif granitique des Zaer (Maroc Central) : minéralisations et phases fluides associées. *Mineral. Deposita*, **19**, 193-203.
- Higgins, N.C. (1985) : Wolframite deposition in a hydrothermal vein system : The Grey River tungsten prospect, Newfoundland, Canada. *Econ. Geol.*, **80**, 1297-1327.
- Ibarrola, E., Villaseca, C., Vialette, Y., Fuster, J. M., Navidad, M., Peinado, M., Casquet, C. (1988) : Dating of hercynian granites in the Sierra de Guadarrama (Spanish System Central). In : *Geología de los granitoides y rocas asociadas del Macizo Hespérico*. Ed. Rueda, Madrid, 377-383.
- Jacobs, G.K. & Kerrick, D.M. (1981) : Methane: an equation of state with application to the ternary system H₂O-CO₂-CH₄. *Geochim. Cosmochim. Acta*, **45**, 607-614.
- Kelly, W.C. & Rye, R.O. (1979) : Geologic, fluid inclusion and stable isotope studies of the tin-tungsten deposits of Panasqueira, Portugal. *Econ. Geol.*, **74**, 1721-1822.
- Kerrick, D.M. & Jacobs, G.K. (1981) : A remodified Redlich-Kwong equation for H₂O-CO₂ and H₂O-CO₂ mixtures at elevated pressures and temperatures. *Amer. Jour. Sci.*, **281**, 735-767.
- Mangas, J. & Arribas, A. (1987) : Fluid inclusion study in the different types of tin deposits associated with Hercynian granites of western Spain. *Chemical Geol.*, **61**, 193-208.
- , — (1988) : Hydrothermal fluid evolution of the Sn-W mineralization in the Parilla ore deposit (Caceres, Spain). *J. Geol. Soc. London*, **145**, 147-155.
- Mangas, J. & Arribas, A. Jr. (1987) : Fases fluidas y metalogenia del yacimiento wolframífero "Virgen de la Encina" (Leon, España). Acta e Comunicações do IX Reuniao sobre a Geologia do Oeste Peninsular. Memórias nº 1, 101-137.
- Massonne, H.J. & Schreyer, W. (1987) : Phengite geobarometry based on the limiting assemblage with K-feldspar, phlogopite and quartz. *Contrib. Mineral. Petrol.*, **96**, 212-214.
- Noronha, F. (1974) : Etude des inclusions fluides dans le quartz du gisement de tungstène de Borralha (Nord Portugal). Publicações do Museu e Laboratorio Mineralogico e Geologico da Faculdade de Ciencias do Porto. LXXXV, 4 serie, 1-36.
- (1984) : Caractéristiques physico-chimiques des fluides associés à la genèse du gisement de tungstène de Borralha (Nord Portugal). *Bull. Minéral.*, **107**, 273-284.
- Noronha, F., Doria, A., Dubessy, J., Charoy, B. (1992) : Characterization and timing of the different types of fluids in the barren and ore-veins of W-Sn deposit of Panasqueira, Central Portugal. *Mineral. Deposita*, **27**, 72-79.
- Potter, R.W. (1977) : Pressure corrections for fluid inclusion homogenization temperatures based on the volumetric properties of the system NaCl-H₂O. *J. Res. U.S. Geol. Surv.*, **6**, 245-257.
- Poty, B., Leroy, J., Jachimowicz, L. (1976) : Un nouvel appareil pour la mesure des températures sous le microscope, l'installation de microthermométrie

- Chaixmeca. *Bull. Soc. fr. Minéral. Cristallogr.*, **99**, 182-186.
- Quilez, E. (1994) : Mineralizaciones filonianas de wolframio de la Sierra de Guadarrama : modelo y caracterización del proceso hidrotermal. Ph. D. Thesis, Univ. Complutense, Madrid, 277 p.
- Quilez, E., Vindel, E., Sierra, J. (1990) : A fluid inclusion study and genetic model of wolframite-bearing quartz veins, Garganta de los Montes, Spanish Central System. *Mineral. Mag.*, **54**, 267-278.
- Quilez, E., Vindel, E., Sierra, J., Dubessy, J., Boiron, M.C., Cathelineau, M. (1991) : Fluid inclusion study of the Cabeza Lijar W-Mo deposit, Spanish Central System. *Plinius*, **5**, ECROFI XI.
- Ramboz, C. (1980) : Géochimie et étude des phases fluides de gisements et indices d'étain-tungstène du Sud du Massif Central (France). Thesis INPL, Nancy, 278 p.
- Ramboz, C., Schnapper, D., Dubessy, J. (1985) : The P-V-T-X-fO₂ evolution of H₂O-CO₂-CH₄ bearing fluid in a wolframite vein : Reconstruction from fluid inclusion studies. *Geochim. Cosmochim. Acta*, **49**, 205-219.
- Roedder, E. (1972) : Composition of fluid inclusions. *U.S. Geol. Surv., Prof Paper*, **440JJ**, 164 p.
- Schenk, P., Holl, R., Ivanova, G.F., Naumov, V.B., Kopneva, L.A. (1990) : Fluid inclusion studies of the Felbertal scheelite deposit. *Geol. Rundsch.*, **79**, 451-466.
- Thiery, R., Vidal, J., Dubessy, J. (1994) : Phase equilibria modelling applied to fluid inclusions liquid-vapour equilibria and calculation of the molar volume in the CO₂-CH₄-N₂ system. *Geochim. Cosmochim. Acta*, **58**, 1073-1082.
- Van den Kerkhof, A.M. (1988) : The system CO₂-CH₄-N₂ in fluid inclusions: theoretical modelling and geological applications. Free Univ. press, Amsterdam, 206 p.
- Velde, B. (1965) : Phengites micas, synthesis, stability and natural occurrence. *Amer. Jour. Sci.*, **263**, 886-913.
- Viallette, Y., Bellido, F., Fuster, J.M., Ibarrola, E. (1981) : Datos geocronológicos sobre el granito de La Cabrera. *Cuad. Geol. Iber.*, **7**, 327-338.
- Villaseca, C., Andonaegui, P., Barbero, L. (1993) : Mapa geológico del plutonismo hercínico de la región central española (Sierra de Guadarrama y Montes de Toledo). Ed. CSIC, Madrid.
- Vindel, E. (1980) : Estudio mineralógico y metalogénico de las mineralizaciones de la Sierra de Guadarrama. Ph D. Thesis, Univ. Complutense, Madrid, 249 p.
- Zhang, Y. G. & Frantz, J.D. (1987) : Determination of the homogenization temperatures and densities of supercritical fluids in the system NaCl-KCl-CaCl₂-H₂O using fluid inclusions. *Chemical Geol.*, **64**, 335-350.

Received 24 March 1994

Accepted 4 January 1995